Factors controlling the age structure of *Margaritifera falcata* in 2 northern California streams

Author(s): Jeanette K. Howard and Kurt M. Cuffey
Source: Journal of the North American Benthological Society, 25(3):677-690.
Published By: The Society for Freshwater Science
DOI: http://dx.doi.org/10.1899/0887-3593(2006)25[677:FCTASO]2.0.CO;2
URL: http://www.bioone.org/doi/full/10.1899/0887-3593%282006%2925%5B677%3AFCTASO%5D2.0.CO%3B2

J. N. Am. Benthol. Soc., 2006, 25(3):677–690

Factors controlling the age structure of *Margaritifera falcata* in 2 northern California streams

Jeanette K. Howard[1] AND **Kurt M. Cuffey**[2]

Department of Geography, 507 McCone Hall, University of California, Berkeley, California 94720-4740 USA

Abstract. Freshwater mussels are long-lived and relatively stationary organisms that form annual rings, so they provide excellent opportunities for studying how population properties such as age structure relate to environmental influences on recruitment and mortality. We investigated population dynamics of the freshwater pearl mussel, *Margaritifera falcata*, in 2 northern California Coast Range rivers, the South Fork Eel and the Navarro. We used field observations and inverse theoretical modeling to assess age structures and identify factors that control population demographics. Distinctly different mortality rates for young (<20 y) and old (≥20 y) mussels were observed in the South Fork Eel, and recruitment and mortality both were related to river discharge regimes. *Margaritifera falcata* recruited more successfully during low-discharge than during high-discharge years, and a 2-fold increase in discharge caused a 60% decline in recruitment success. Active annual recruitment (~1100–1800 ind./y) was observed in the South Fork Eel, whereas recruitment has been low or nonexistent during the past 30 y in the Navarro. This difference probably is a consequence of the influence of 2 non-mutually exclusive factors: landuse history and host-fish abundance. The Navarro watershed has extensive timber harvesting and orchard/vineyard agriculture and has had severe declines in fish populations, whereas large sections of the South Fork Eel pass through protected land and the river has retained its historical fish populations. Investigation of the factors that shape local *M. falcata* population age structures yielded insights into the influence of environmental variables and history on mortality and recruitment that will aid conservation of this endangered family.

Key words: freshwater mussels, age structure, California, *Margaritifera falcata*, discharge, recruitment, mortality, annual rings.

The worldwide decline of freshwater mussels has been the focus of many studies over the past decade. Alarming losses of species and of numerous populations have been documented, and >70% of freshwater mussel species are imperiled or extinct (Butler 1989, Williams et al. 1992, Neves et al. 1997, Brim Box 1999, Brim Box and Williams 1999). Extinction rates for freshwater mussels are an order of magnitude higher than expected background levels (Nott et al. 1995), so a comprehensive understanding of environmental influences on freshwater mussel population dynamics is essential for conservation efforts.

Freshwater mussels provide excellent opportunities for population ecology research. A major goal of population ecology is to quantify population processes, such as mortality and recruitment, in concert with population characteristics such as age and density (Renshaw 1991, Cappuccino and Price 1995, Kingsland 1995, Caswell 2001, Oli 2003). Mussels are particularly useful models in this context because they have annual rings, making it possible to determine the population age structure at specific points in time. In addition, mussels are long-lived and relatively stationary; thus, they can provide a cumulative indication of long-term environmental conditions at a site of interest (Nystrom et al. 1996).

Scattered information is available on the population demographics of freshwater mussels. Previous studies have focused primarily on growth characteristics (Hendelberg 1961, Stober 1972, Bauer 1983, 1992, Day 1984, Hruska 1992, Toy 1998, Hastie et al. 2000a), descriptions of population age structure (Hendelberg 1961, Hruska 1992, Hastie et al. 2000b), or the use of shells as environmental recording devices (Carell et al. 1987, Aberg et al. 1995, Nystrom et al. 1996). Together, these studies have provided insight into mussel demographics, but only a few studies have quantified vital rates, such as mortality and recruitment, that affect population age structure (Bauer 1983, 1992).

We used an inverse theoretical technique to analyze

[1] E-mail addresses: jeanette.howard@gmail.com

[2] kcuffey@berkeley.edu

population age structure and identify environmental factors controlling demographics of the western pearly-shell mussel, *Margaritifera falcata* (Gould 1850), in 2 rivers in the northern California Coast Range. This analysis uses measured values of some characteristic (e.g., age) and combines them with a mathematical description of processes to infer values of unmeasured parameters (e.g., recruitment, mortality) (Menke 1989). Inverse theoretical modeling provides estimates of mortality rates and information about their variation with age, and it can reveal whether temporal variation in mortality and recruitment is related to environmental factors such as river hydrology and recent land use in the watershed. Our main objectives were to: 1) determine the age structure of *M. falcata* populations in 2 rivers with contrasting landuse histories, 2) determine growth rates of individual mussels as a function of age, 3) quantify population mortality and recruitment rates, 4) identify the degree to which temporal variation in recruitment and mortality determine age structure, and 5) determine if these population parameters were related to environmental variables.

Two environmental variables may be particularly important factors controlling mussel recruitment and mortality in streams in the North Coast Range. Mussels in these streams typically inhabit low-shear-stress regions of channels (Howard and Cuffey 2003), but interannual variability in flood discharge magnitude can be high and is influenced by El Niño (high mean discharge) and La Niña (low mean discharge) in some years and may affect both recruitment and mortality. In addition, host-fish abundance may determine recruitment because mussel larvae must parasitize fish early in their life cycle (Coker et al. 1921). Thus, the dramatic 20th-century decline of anadromous fish in California rivers could have reduced mussel recruitment substantially.

Methods

Study sites

We quantified age structure of *M. falcata* in portions of the South Fork Eel and the North Fork Navarro rivers in California, USA (see Howard et al. 2005 for map). The South Fork Eel River is part of the 9000-km^2 Eel River system, the 3rd largest river system in California. The South Fork Eel watershed (1783 km^2, 30–1370 m asl) is ~ 270 km from San Francisco, and the South Fork Eel River flows north from its headwaters for ~160 km before it joins the mainstem Eel River, which continues for ~64 km to the Pacific Ocean near Humboldt Bay. Our study area is in a 4th-order channel with a mean gradient of 0.0044. A well-defined alternating pool–riffle structure is present in the stream. Much of the study area lacks a floodplain, and the stream bed is dominated by incised cobble river terraces and bedrock. Some logging occurred in the watershed from the early to mid 1900s, but the study area has been protected as a conservation site since 1959, and it is now known as the Angelo Coast Range Reserve, part of the University of California's Natural Reserve System.

The Navarro River watershed (815 km^2, 0–760 m asl) is ~190 km north of San Francisco. The Navarro River flows northwesterly through the coastal range and the Anderson Valley to the Pacific Ocean. Our study area was in the North Fork Navarro River subwatershed and the lower reaches of the Navarro River. The study area is in a 3rd-order channel and drains 190 km^2 (mean gradient = 0.0041), and includes the entire North Fork Navarro River watershed from its headwaters to its confluence with the Navarro main stem. Unlike the South Fork Eel site, the Navarro watershed underwent massive landuse changes following the start of timber harvesting in the mid 1800s. A 2nd logging boom occurred from the late 1930s to the early 1950s, when large tracts of redwood-dominated forest in the mainstem Navarro River subwatershed were reharvested (Entrix et al. 1998). Current land uses in the Navarro watershed are commercial timber harvesting, grazing, viticulture, and orchards (Entrix et al. 1998). In addition, State Highway 128, constructed between 1933 and 1963, runs parallel to the river for most of its course through the Anderson Valley.

Study species

Margaritifera falcata is restricted to regions west of the Continental Divide and has been reported from many Pacific watersheds from southern Alaska to central California (Taylor 1981). The mussel and its eastern relative, *M. margaritifera*, are long-lived species (individuals may live for >100 y; Bauer 1992, Hastie et al. 2000a, b). Like most unionid mussels, *M. falcata* has an obligate parasitic larval stage on fishes. After completing larval development, juvenile mussels drop from their hosts onto the river bed and become minute (~60-μm) free-living bivalves. The length and timing of *M. falcata's* parasitic cycle is currently unknown. Host fish include chinook salmon (*Oncorhynchus tschawytscha*), rainbow trout (*O. mykiss*), coho (*O. kisutch*), cutthroat trout (*Salmo clarki*), and steelhead trout (*S. gairdneri*) (Fuller 1974, Karnat and Millemann 1978).

Mussel surveys

We surveyed mussels during spring and summer 2000 and 2001 in an 8-km reach of the South Fork Eel

River (Howard and Cuffey 2003, Howard 2004) and in a 10-km reach of the North Fork Navarro and Navarro main stem. We resurveyed the 5 largest populations in the South Fork Eel study area in summer 2003. We searched for mussel aggregations (i.e., $\geq$10 individuals) by snorkeling and wading in shallow reaches and diving in the deepest pools. We found 114 *M. falcata* aggregations totaling ~12,000 individuals in the South Fork Eel (Howard and Cuffey 2003), whereas we found only ~350 individuals in the Navarro River.

We selected a subset of mussel aggregations in the South Fork Eel study area for more detailed measurements of shell lengths. We selected all large aggregations (>500 mussels, $n = 11$) and randomly selected additional aggregations in the study areas to ensure adequate spatial coverage (i.e., the longest linear distance between sampled aggregations was <500 m). We measured shell lengths along the maximum growth axis (to the nearest 0.5 mm) of all mussels occurring within randomly placed 0.5-m^2 quadrats in each aggregation. We used enough quadrats to ensure that $\geq$10% of the individuals in aggregations with >300 individuals were measured. We measured $\geq$50% of the individuals in small aggregations (<300 individuals). We measured all visible mussels in each quadrat, and we excavated and sieved (2-mm mesh) the upper 10 cm of substrate in the quadrats to detect small (<10 mm) individuals. Fewer than 0.5% of the individuals in the quadrat were obtained from excavated substrate.

In the South Fork Eel, we measured 2,050 and 865 mussels in 2000 and 2003, respectively, whereas we measured all mussels in the Navarro River ($n = 315$). We returned all mussels measured to their collection site.

Age determination

We collected 90 *M. falcata* from a total of 4 sites along the South Fork Eel River and 15 individuals from 1 site on the north branch of the Navarro River in August and September 2002 and 2003 for age determinations. We allowed mussels to evacuate their gut contents in fresh water for 48 h, rinsed them in fresh water, and then froze them (–5°C) until they were processed.

We used a diamond saw to section shells, which were cut from the umbo region to the ventral margin, following the vector of maximum growth. We mounted sections on glass slides with epoxy and vacuum-sealed them into a vice attached to the cutting arm of the saw. We reduced the thickness of sections (~250 µm wide) by sanding them with successively smaller grit sizes and polished them with fine lapidary powders (3-µm and 1-µm-diameter grit sizes; Neves and Moyer 1988). Thickness of the finished sections was between 150 and 200 µm and provided the necessary translucence for detection of growth bands. Growth increments are continuous from the prismatic layer to the external nacreous sublayer and appear as light bands (areas of high seasonal growth) interspersed by dark narrow lines (areas of low [winter] growth). We counted annual rings and measured interannular growth distances under a compound microscope (10–40×). We counted each thin section 5 times to ensure accuracy.

Confirmation of annual growth identifiers

We notched, measured, and labeled 100 *M. falcata* shells during summer 2000 in the South Fork Eel to ensure that the dark lines visible in thin sections indicated annual growth. We removed mussels from the substrate and measured the length (nearest 0.5 mm) and mass (nearest 0.1 g) of each mussel. Before we returned a mussel to the substrate (within 15 min of removal), we used adhesive (Devcon Super Glue™) to attach Bee Tags™ labels to the left valve, and filed a notch on the left ventral margin of one valve. We used notches to mark the shell edge. The notches allowed us to count annual rings produced after marking when mussels were collected in subsequent years. We recovered subsamples of marked mussels ($n = 13$) in the summers of 2002 and 2003 and prepared thin sections as above to verify accuracy of annular growth increments. Subsequent examination of thin sections demonstrated conclusively that growth increments were annual.

Calculating ages from length measurements

We plotted age against shell length and used least-squares optimization to fit 3 nonlinear growth curves (power, exponential growth to maximum age, logarithmic; Hastie et al. 2000a) to the shell length-at-age data (Fig. 1). The best fit was to the standard 3-parameter logarithmic equation:

$$L = L_o + a \ln(A - A_o) \qquad [1]$$

where L is length of the mussel shell, A is age, and a, A_o, and L_o are constants. We used the inverse of this equation to calculate ages for all measured mussels.

Accounting for variability in the length–age relationship and age histograms

Two mussels of the same length could be different ages, thereby causing uncertainty in our age determinations based on length. Examination of the deviations from the best-fit logarithmic model showed that this uncertainty increased with age, and was approximately ±1 y for shells <50 mm, ±2 y for shells between 51 and 56 mm, and ±3 y for shells >57 mm.

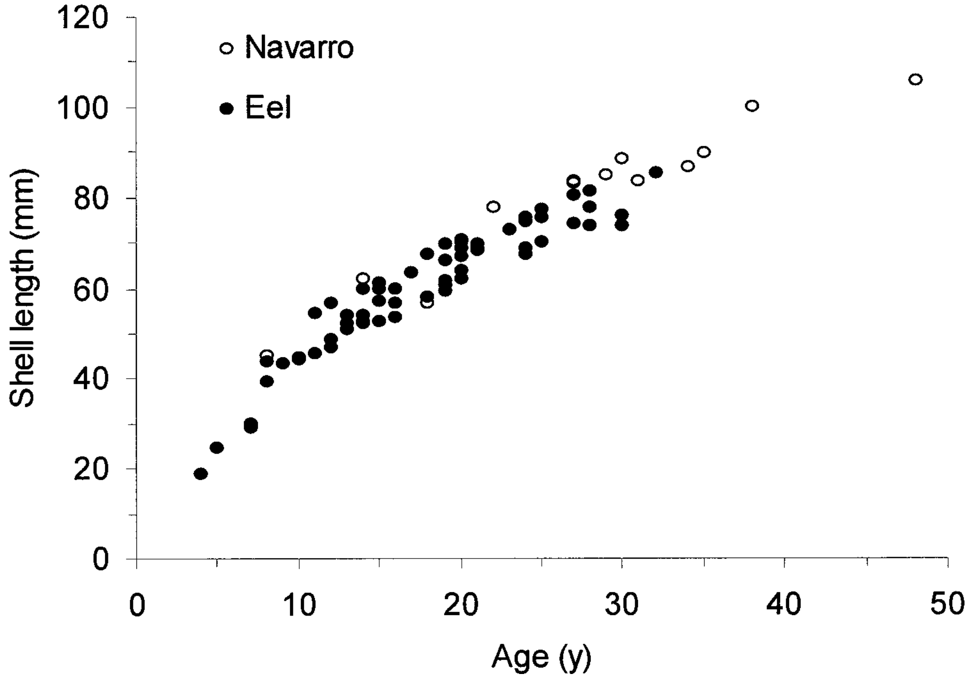

Fig. 1. Relationship between measured age and shell length of the freshwater mussel *Margaritifera falcata* from the South Fork Eel and the North Fork Navarro rivers, California.

We incorporated this uncertainty directly into the age histograms. For example, age of a mussel of 60-mm length would be estimated as 17 y from the best-fit model. Given the ±3 y uncertainty on this age, we assumed that the true mussel age was between 14 and 20 y, with equal probability for all of these ages. We proportionately scaled the contribution of this one mussel to the various classes in the age histogram to ensure that all individuals had equal weighting despite variations in the uncertainty. The uncertainty on ages of older mussels might have been larger than the ±3 y estimated from the data ranges (Fig. 1). For example, erosion of annual layers from shells could cause our thin-section counts to be underestimates of true age. In our analysis of model parameter uncertainty (see below), we increased the error estimate of age for these mussels by an additional ±10% (e.g., ±7 y for mussels of estimated age 40).

We constructed histograms from all of the individual age estimates, accounting for age uncertainty as discussed above, for each mussel aggregation measured in 2000 and 2003. We also combined these estimates into population-weighted age histograms for the entire South Fork Eel and Navarro study sites.

Recent mortality rates

We compared age histograms from 2000 and 2003 to obtain direct information about recent mortality rates. We used a standard definition of annual mortality rate (α), as:

$$\frac{dN(t)}{dt} = -\alpha N(t) \qquad [2]$$

where $N(t)$ is the number of mussels in an age class at time t. Thus, the number of mussels alive in 2003 was a function of the number in 2000 according to:

$$N(2003) = N(2000)\exp(-3\alpha_3) \qquad [3]$$

where α_3 is the 3-y mean of α. Using our data, we then calculated α for each age class using:

$$-\frac{1}{3}\ln\left(\frac{N(2003)}{N(2000)}\right) = \alpha_3 \qquad [4]$$

We plotted α_3 against age to determine whether mortality varies systematically with age. We also examined the plots for negative values for α_3, which would indicate major problems with the constructed age histograms.

Methods for analysis of population age structure

We designed analyses of age-structure data to yield information on mean mortality and recruitment rates, their variations over time, and their relationships with environmental variables. We used a standard approach from inverse theory (Menke 1989, Press et al. 1992) to model calculations of age structures and

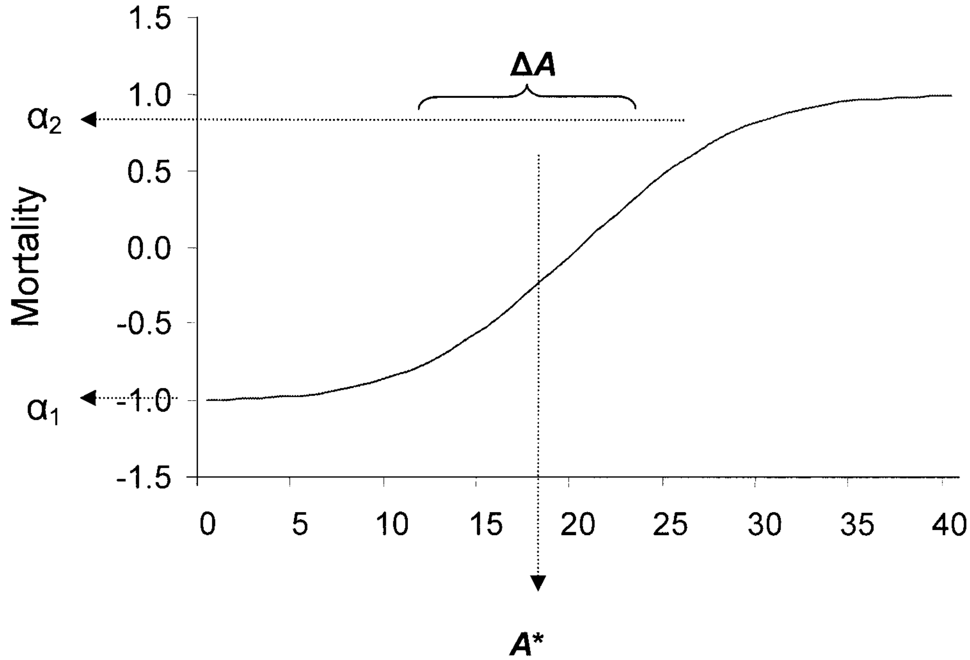

FIG. 2. Form of the mortality vs age function (α) used in the analyses (eq. 7) with arbitrary 0. Parameters α_1 and α_2 were calculated by analysis of age histograms. Parameters ΔA and A^* were estimated from 3-y mortality data.

compare them to measured age structures; we used the least-squares optimization to find best-fit models for unknown model parameters (Press et al. 1992). We then used a Monte–Carlo technique to validate conclusions and define uncertainties for model parameters. We used 3 models with successively higher numbers of unconstrained parameters (3-, 4-, and 5-parameter models, see below) to find the best-fit model. We measured model performance using a standard least-squares index (J), defined by:

$$J = \frac{1}{(A_{\max} - A_{\min})} \sum_{j=A_{\min}}^{A_{\max}} (Nj^{\text{measured}} - Nj^{\text{modeled}})^2 \quad [5]$$

where N_j is the number of individuals in the j^{th} age class, and the sum of the squared differences between Nj^{measured} and Nj^{modeled} is taken over all ages of the population from $A_{\min}$ to $A_{\max}$, with $A_{\min} = 6$ for the South Fork Eel (see Results for justification for this value of $A_{\min}$). Optimal values for the model parameters were those that minimized J. The minimization was accomplished using iterative application of Singular Value Decomposition (SVD, Appendix 1). We did optimizations on histograms for all mussels in the South Fork Eel and Navarro rivers.

Analysis 1 (3-parameter model): time-invariant recruitment and mortality.—We asked what information could be extracted from the age histograms assuming no variation of mortality and recruitment over time. We used a model incorporating 3 unknown parameters: 1) youthful (<20 y) α_1, 2) adult ($\geq$20 y) α_2, and 3) mean recruitment rate. We used eq. 3 to calculate the number of mussels (N_y (t)) born in year y that were living in year t as:

$$N_y(t) = N_o \exp\left[-\int_{t-y}^{t} \alpha(t-y)dt\right] \quad [6]$$

where N_o is the recruitment rate.

We incorporated variation of α with age based on results from the analysis of recent values of α (see Results, *Recent mortality rates*). We used 2 independent parameters as limiting values for mortality (α_1 and α_2 for youth and old age, respectively), and specified α using the functional switch (Fig. 2):

$$\alpha(A) = \left[\left(\frac{\alpha_2 - \alpha_1}{2}\right)\operatorname{erf}\left(\frac{A - A*}{\Delta A}\right)\right] + \left(\frac{\alpha_1 + \alpha_2}{2}\right) \quad [7]$$

where erf is the error function, A = age (equivalent to $t - y$), A^* and ΔA are both constants, estimated from the 2000 to 2003 comparison (see Results, *Recent mortality rates*), A^* = age at which the mean of α_1 and α_2 is attained, and ΔA = the time interval for the switch from α_1 to α_2. We estimated values for the parameters A^* and ΔA from the data (Fig. 3) and did not allow these values to vary or to be optimized. Thus, only the parameters N_o (eq. 6), α_1, and α_2 were optimized.

Analysis 2 (4- and 5-parameter models).—Deviations of the 3-parameter model from measured age histograms

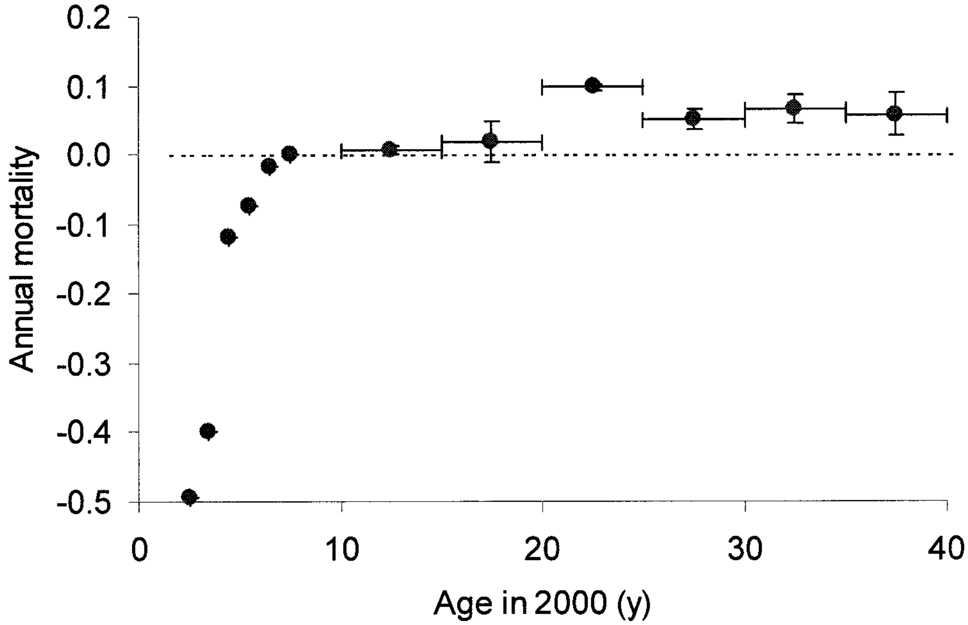

FIG. 3. Relationship between *Margaritifera falcata* mortality averaged over 5-y intervals and mussel age. Negative values at ages <5 y indicate undersampling of juveniles.

reflect temporal variation in recruitment or mortality. Results from Analysis 1 suggested that such variations were significant and were related to variations in river discharge (see Results, *Analysis 1*). Therefore, we also used models containing additional parameters to test this relationship. We assumed that high flows influence mussel survivorship more than low flows (Howard and Cuffey 2003) because the highest channel-bank shear stresses occur when discharge (Q) is highest. For this reason, we defined an index of high Q magnitude (Q^*_n) as the mean of the largest 5% of all flows in an n-year period. We calculated this index using gauging station data (Appendix 2), and then averaged Q according to the uncertainty in estimated ages for the corresponding year. We used $n = 2$ in our calculation because it gave the best correlation between Q and the nominal recruitment calculated in Analysis 1. This value is equivalent to claiming that the largest floods experienced within 2 y of birth were the greatest threat to juvenile mussel survival. We specified that N_o varied only as a function of Q, with a single constant b defining the sensitivity:

$$N_o(y) = r_o\left(1 + b\left(\frac{Q^*_n(y)}{\overline{Q}^*_n} - 1\right)\right) \qquad [8]$$

where r_o is the mean recruitment rate, and $\overline{Q}^*_n$ is the mean of Q^*_n for entire data set.

We also asked whether mortality was influenced by Q by including an additive perturbation to α as:

$$\alpha^*(t, t-y) = \alpha_0(t-y) + \mu\left(\left(\frac{Q^*_n(t)}{\overline{Q}^*_n}\right) - 1\right)$$
$$\alpha(t, t-y) = \max\big(0, \alpha^*(t, t-y)\big) \qquad [9]$$

where μ = sensitivity of mortality to Q and α_0 is the mortality rate calculated from eq. 7. We optimized 5 parameters (α_1, α_2, r_o, b, and μ) in this analysis. We also examined optimized models with only the 4 parameters α_1, α_2, r_o, and b, and compared the mismatch to that for the full 5-parameter model to evaluate the importance of b relative to μ.

Evaluation of uncertainties for optimized model parameters.—We evaluated the statistical significance of each optimized model parameter for the 5-parameter model. We used a Monte–Carlo technique to answer 2 questions about model parameters: 1) What are the 95% confidence intervals for each optimized model parameter?, and 2) Does each model parameter contribute significantly to describing the age structure of the populations? This procedure was equivalent to asking whether the optimized parameters were different from 0, a question that could be answered implicitly by inspecting the size of the confidence intervals.

We randomly perturbed uncertain model inputs and then recalculated optimal parameter values. We repeated this process ~500 times and then assembled the optimal values into frequency distributions. The model had 4 significant potential sources of error: 1) Q,

2) the fixed parameter ΔA, 3) the fixed parameter A^*, and 4) the age histograms. Perturbations to these parameters were as follows: 1) Q—We multiplied Q values by a normal random variable with mean = 1 and a standard deviation (SD) = 0.02 to obtain an 8% range of Q perturbations, commensurate with the covariance of gauging station data at Branscomb and Leggett (Appendix 2). 2) Fixed parameters ΔA and A^*—We multiplied parameter values by normal random variables with mean = 1 and SD = 0.05 to obtain a ±2 SD interval of 4 y for A^*, which was reasonable given the data (Fig. 1). 3) Age histograms—We perturbed values with a 6-y sinusoidal wave function with a random phase and an amplitude that decreased as a function of age (i.e., the value of the perturbation as a % of the nominal histogram value increased from 5% at age 0 y to 10% at 40 y). This choice for the uncertainty was based on a Monte–Carlo estimate of the mismatch between a frequency distribution given exactly by the measured distribution and a random subsample of 2050 (*n* for measured mussels) taken from this distribution. We compared the measured distribution to 1500 subsampled distributions to compile the uncertainty estimate.

Evaluation of predictive power.—Incorporating Q data into the optimization analysis led to significant improvements in the match between modeled and measured age histograms. We did a 2nd Monte–Carlo analysis to determine if this improved match occurred because of our optimization procedure and analysis or because the Q data had genuine predictive power. We randomly fabricated discharge time-series data, assuming Q was distributed as a uniform, random variable with upper and lower limits given by the real Q data. We treated each of these fabricated Q sets identically to the real data (converted to a Q_n^* time series, and then used the time series to calculate optimized parameters). We repeated this step ~1000 times to compile a frequency distribution of the mismatches (J), and then compared the mismatch associated with the real Q data to this distribution.

Results

Age histograms

Mussels were abundant (>12,000 individuals; Howard and Cuffey 2003) in the South Fork Eel sites sampled and included a substantial number of younger individuals (Fig. 4A). Less than 16% of the population was ≥20 y old, with the oldest individuals ranging between 33 and 39 y. Few individuals <6 y old (juveniles) were found in 2000. However, this low number of juveniles was a sampling artifact, as indicated by comparing the 2000 and 2003 age distributions (Fig. 4A). If the number of juveniles found in 2000 had been accurate, the mid-juvenile portion (ages 3–9) of the 2003 distribution should have been a right-shifted version of the 2000 distribution. Instead, the 2003 histogram reflected the 2000 histogram up to age 5, but the number of individuals in the 5 to 9 age classes in the 2003 histogram was similar to the number of individuals in the age 5 age class in the year 2000 histogram (Fig. 4A). The upper peaks of the 2 histograms were similar (ages 6–12 in year 2000, ages 9–15 in 2003; Fig. 4A), demonstrating that this age-distribution shift was a real feature of the population age structures. In 2000, the histogram peaked between ages 8 and 11, whereas in 2003 the peak occurred between ages 11 and 14.

Recent mortality rates

Estimated α_3 was negative for ages 1 to 5 (Fig. 3) and clearly showed that the scarcity of juveniles in 2000 was a sampling artifact. Given this result, $A_{min} = 6$ was selected for subsequent analyses (in eq. 7). The plot of α_3 against age in 2000 showed a higher mortality rate for adults (≥~20 y) than for younger mussels, whose α_3 values were ~0 (Fig. 3). This result motivated the form of eq. 7. The plot of α_3 against age showed that mortality rate varied with age. However, the inferred age-specific mortalities may be uniformly offset from their true values because the age histograms were subsamples of the total population, and total population size may have changed during the 3-y study. This offset was unlikely to be significant given the close match of the population peak in both years (Fig. 4A).

Population age structure

Analysis 1.—The optimized, time-invariant (3-parameter) model reproduced key features of the age histogram of the South Fork Eel population (Fig. 5); however, a considerable mismatch between the modeled and actual histograms still existed. Optimal values for the model mortality parameters were 0.04 and 0.22/y for juveniles and adults, respectively, r_o = 1200 mussels/y or 0.15 mussels y^{-1} m^{-1} channel length.

Deviations from this time-invariant model probably were the result of annual variations in r_o. A perfect match between modeled and measured histograms could be achieved if r_o varied as shown in Fig. 6A, with a quasicyclical pattern of high and low nominal recruitment. High recruitment occurred between 1976 and 1978 and between 1987 and 1992, whereas low recruitment occurred between 1980 and 1986 and 1991 and 1994 (Fig. 6A).

Analysis 2.—Incorporating Q data in the population

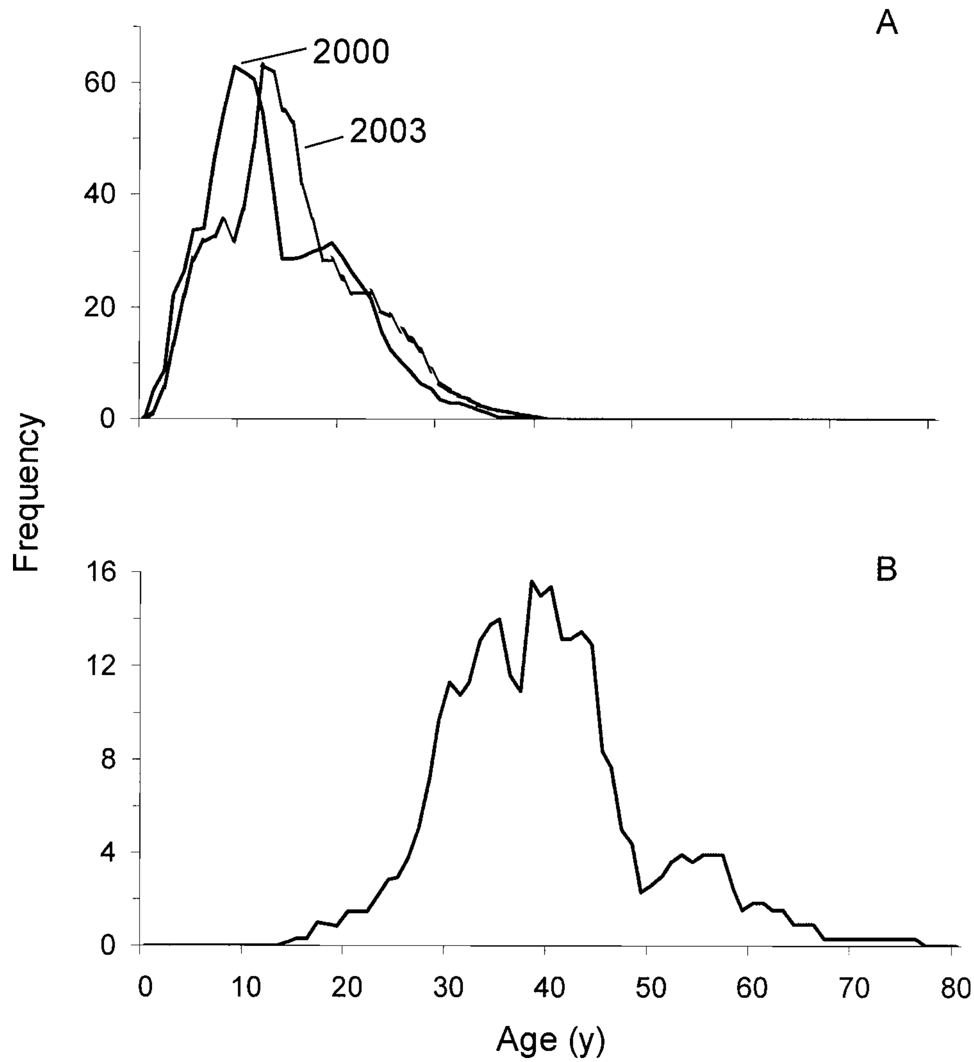

FIG. 4. Population age histograms for *Margaritifera falcata*. A.—The South Fork Eel River in 2000 and 2003. B.—The North Fork Navarro River in 2003.

model provided a much better result than the 3-parameter model (Fig. 5), with a significantly lower J. Most of the improvement resulted from inclusion of the Q-dependence of recruitment (non-0 b). Relative to the 3-parameter model, J was reduced by a factor of 2.5 using the 4-parameter model (α_1, α_2, r_o, b), and inclusion of the Q-dependence of mortality (5-parameter model) yielded further improvement, although this increase only was marginally important (J was reduced by 23% relative to J for the 4-parameter model; Fig. 5). The sensitivity of recruitment to Q (4-parameter model) yielded $b = -0.60$, implying that a doubling of Q decreased recruitment by 60%. Mean r_o (= 1400 mussels/y) for the 5-parameter model and youthful and adult mortalities were comparable to previous results (0.02 and 0.18/y, respectively). An important point is that Q-dependent mortality did not significantly change the inferred sensitivity of r_o to Q ($b = -0.59$). The optimized sensitivity of mortality was $\mu = -0.15$/y, implying that mortality was lower (and N_o was lower) in high-Q years than in low-Q years.

Evaluation of uncertainties for optimized model parameter

Four of the model parameters (α_2, r_o, b, μ) significantly shaped the age structure of the population in the South Fork Eel River. Youthful mortality was indistinguishable from 0 and was much lower than adult mortality; measurements of mussel lengths (converted to ages) from 2000 to 2003 in the field corroborated this result independently (Figs 3 and 4).

The sensitivity of r_o to Q ($b = -0.59$) was closely constrained between -0.5 and -0.7 (Table 1). In

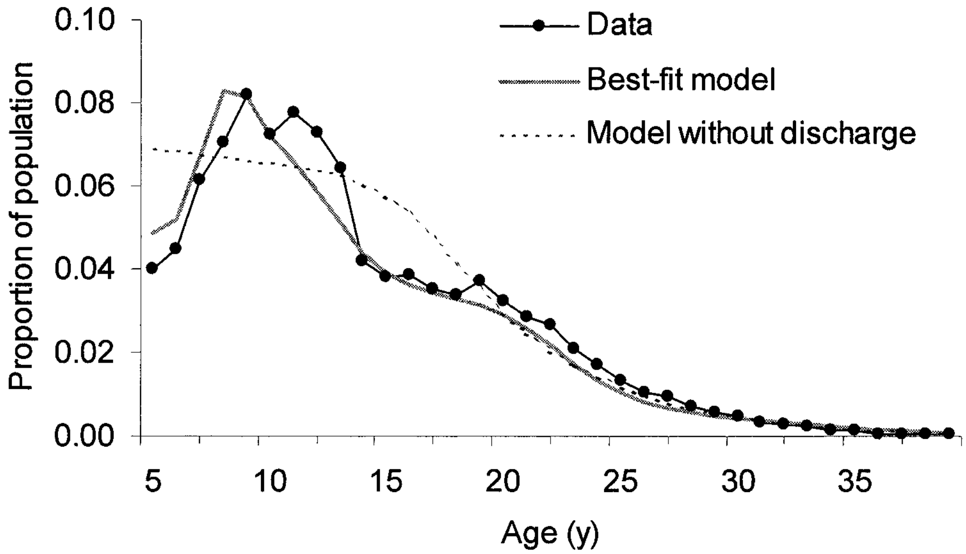

FIG. 5. Comparison of the 5-parameter (best-fit model) and the 3-parameter (model without discharge) optimized model for *Margaritifera falcata* in the South Fork Eel River plotted with real age histogram data.

contrast, the sensitivity of mortality to Q was less well constrained but still demonstrably negative (Table 1).

Evaluation of predictive power

The real Q data provided a better match between modeled and measured histograms than did >95% of the random Q time series (Fig. 7), indicating that our optimization procedure probably did not force the results discussed above. Instead, the impacts of Q on recruitment and mortality were significant factors altering *M. falcata* population structure.

Navarro River results

Margaritifera falcata were much less abundant (only ~350 individuals in 5 aggregations) and individuals were considerably older (99% of the Navarro population ≥20 y; Fig. 4B) in the Navarro than in the South Fork Eel. The oldest mussels were between 70 and 76 y. The apparent peak of the population occurred at 38 y. The low number of mussels born after 1972 (28 y old) and the absence of mussels born after 1989 (in the past 14 y) were particularly striking. The population age structure of *M. falcata* in both rivers was characterized by an exponential decrease in the frequency of older individuals. In the Navarro, a best-fit exponential to the declining limb of the age distribution gave an estimate for adult mortality of ~0.09, a value much lower than adult mortality at the South Fork Eel (0.2). The Navarro age distribution was perfectly matched by calculating a nominal r_o from the ratio of the data to the best-fit exponential model as shown in Fig. 6B.

Discussion

Apparent absence of juvenile mussels

The apparent scarcity of juvenile (<6 y old) *M. falcata* in the South Fork Eel was an artifact; our resampling of study sites demonstrated conclusively that many of the juvenile mussels alive in 2000 (i.e., found in 2003) were not detected in 2000 (Fig. 4). We do not know the reason for our inability to detect juveniles in the South Fork Eel. One possibility is that juveniles and adults were distributed in different microhabitats within the channel, or they may have burrowed deeper in the substrate than we excavated (10 cm), making them difficult to find (Hastie et al. 2000b). *Villosa iris* burrowed ~1 cm within 20 min of placement on the substrate (Yeager et al. 1994), and *M. falcata* has been observed burrowing within 15 min of being placed on both gravel and sand substrates (JKH, personal observation). Another possibility is that juveniles were too small to be detected in our surveys (Hastie et al. 2000b). Small sizes (glochidia are ~60 μm long) may have contributed to our inability to find juvenile *M. falcata* (JKH, personal observation). However, 2- to 4-y-old mussels in the South Fork Eel were between 10–24 mm in length and were easily recognizable in the channel (JKH, personal observations).

In contrast, young mussels (>10 y, age classes that were easily detected in the South Fork Eel) truly were absent from the Navarro. The absence of juveniles in the Navarro could be explained by some mortality event that affected only younger mussels, but a more plausible explanation is that the r_o varied as shown in

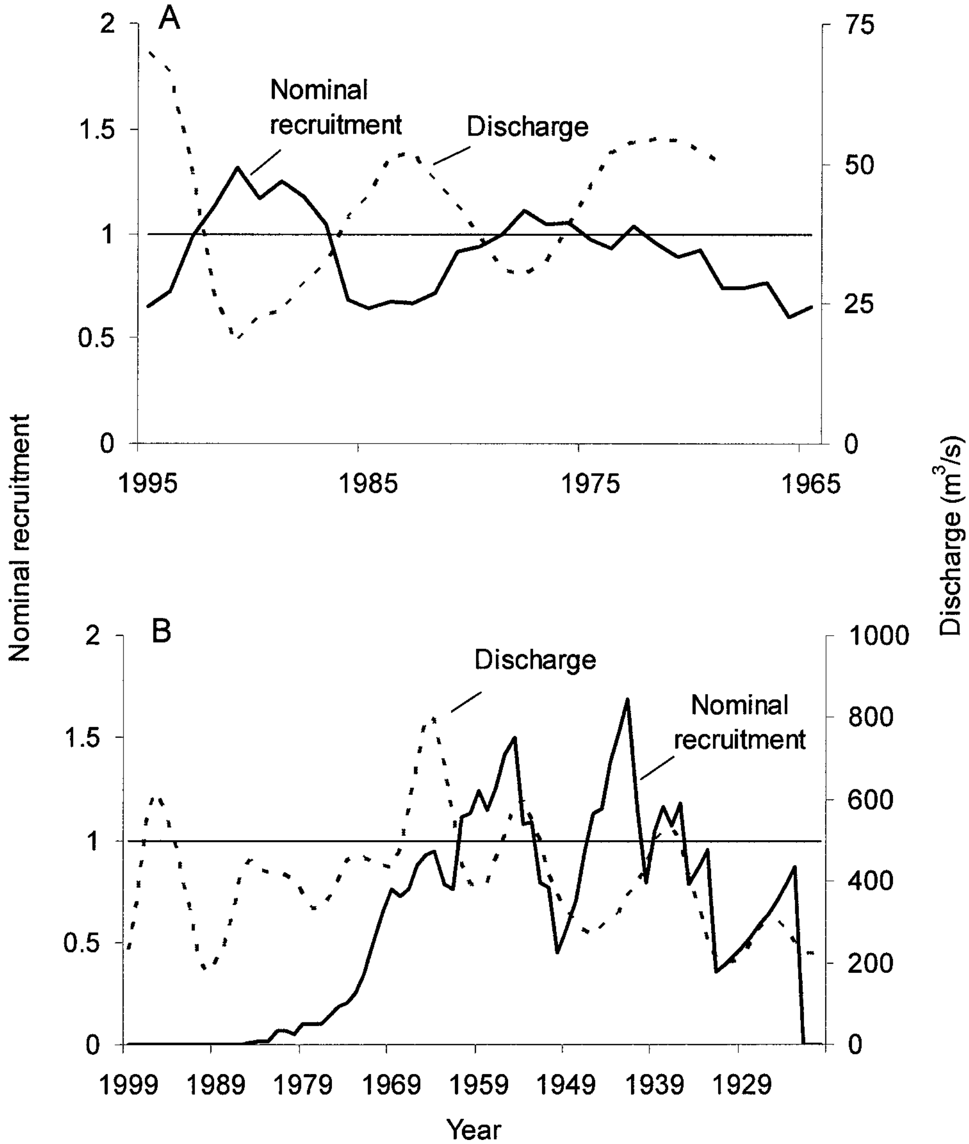

Fig. 6. Relationship between nominal recruitment rate of *Margaritifera falcata* and discharge of the South Fork Eel River (A) and the North Fork Navarro River (B). Nominal recruitment is the ratio between the real and modeled histograms and is the recruitment rate necessary to achieve a perfect match to the mussel age data.

Fig. 6, with serious decline beginning before 1970 and complete failure occurring after 1984. Anomalous *Q*s over the past 2 decades did not explain the observed recruitment failure in the Navarro (Fig. 6B). Extremely low numbers or total absence of juveniles resulting from declining recruitment have been reported for other mussel species in other rivers (Hendelberg 1961, Bauer 1983, Beasley and Roberts 1999).

Mortality rates

Empirical data and modeling results indicated 2 distinct mortality rates for *M. falcata* in the South Fork Eel: 1) following high initial mortality rates for very young mussels at a rate not quantified here, juvenile (5- to 20-y-old) mortality of ~2%, and 2) a 15 to 20% mortality rate for mussels >20 y. The latter mortality rate accounted for the exponential decline in older individuals in the South Fork Eel. Bauer (1983) reported similar results for *M. margaritifera* in a North Bavaria river, where mortality for mussels <40 y old was nearly 0 and mortality for mussels >40 y old was ~20%. In our study, adult mortality was much lower in the Navarro than the South Fork Eel (0.09 and 0.2/y, respectively), a difference that accounted for the presence of substantially older individuals in the Navarro than in the South Fork Eel.

TABLE 1. Optimal values of 5 life-history parameters for the freshwater mussel *Margaritifera falcata* obtained from analysis 3 (see text) and the 5^{th} and 95^{th} percentile confidence limits.

Parameter	Optimal value	5^{th} percentile	95^{th} percentile
Youthful mortality	0.02	–0.002	0.033
Adult mortality	0.18	0.16	0.21
Mean recruitment rate	0.12	0.09	0.15
Sensitivity of recruitment to discharge	–0.59	–0.50	–0.64
Sensitivity of mortality to discharge	–0.15	–0.10	–0.19

The present number of observed old-age mussels in the Navarro River could be explained by an r_o of ~80 mussels/y in the 1940s and 1950s, assuming the application of the adult mortality rate for mussels >20 y in the South Fork Eel to the mussels in the Navarro. This value is comparable to total mussel recruitment in a ~300-m reach of the modern South Fork Eel. We found all Navarro mussels within a single 500-m reach, suggesting that mussel recruitment in this section of the Navarro in the 1940s and 1950s was comparable to recruitment in the present-day South Fork Eel.

Environmental controls on age structure

Population dynamics of *M. falcata* were associated with environmental conditions, most notably annual river discharge regimes. r_o was strongly dependent on the magnitude of Q, and recruitment was significantly reduced in high-discharge years. A striking example of low recruitment occurred during 1991 to 1994 (Fig. 6A), a particularly strong El Niño period (Western Regional Climate Center 2002). Discharge in rivers along the north coast of California increases during El Niño periods, a pattern that suggests that mussel recruitment in coastal California rivers may decrease in El Niño years. Our analyses provide weak evidence for a suppression of mortality of established mussels during high-discharge years, and this lower mortality may, in part, counteract decreased recruitment during high-discharge years.

At least 3 potential mechanisms could account for the high-discharge–low-recruitment pattern. First, juvenile mussels may be displaced downstream by flow. Mussels in the South Fork Eel typically occur in parts of the channel where shear-stress magnitude is minimized, making displacement during floods less likely (Howard and Cuffey 2003). Shear stress is correlated with discharge, so juvenile mussels may be more likely to be displaced during high-flow events than at other times. In a related study of abundance of *M. margaritifera* before and after a 100-y flood, 4 to 8% of the population was killed as a result of the flood (Hastie et al. 2001). Mussels were displaced considerable distances downstream from preflood locations, and the youngest age classes (<10 y) were most affected. Second, host fishes for *M. falcata* are salmo-

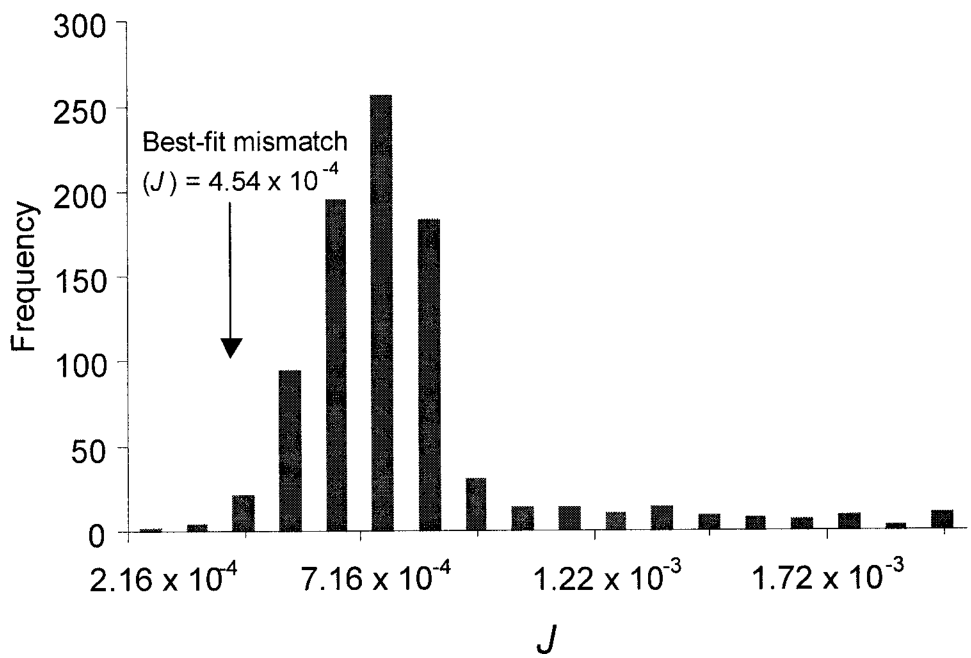

FIG. 7. Distribution of the model mismatch indices (J) obtained with 1000 permutations of fabricated random-discharge time-series data. The arrow indicates the best-fit mismatch achieved with the real discharge time-series data.

nids (see *Study species* above; Karnat and Milleman 1978), and juvenile salmonids are considered more important hosts than adults because salmonids develop immune responses to glochidial infection that reduce glochidal survivorship (Karnat and Millemann 1978, Bauer and Vogel 1987). High-discharge events cause emigration and mortality of overwintering juvenile salmonids (McMahon and Hartman 1989, Giannico and Healey 1998), so low mussel recruitment in high-discharge years may be an indirect effect of reductions in juvenile salmonid abundance in high-discharge years relative to low-discharge years. Last, high-flow events may reduce stream temperatures (Younus et al. 2000), and low temperature has been linked with reduced recruitment success in freshwater mussels (Hruska 1992) because most species require a thermal threshold to begin spawning (Dillon 2000).

Discharge-dependent mortality

Unlike juveniles, adult *M. falcata* are not adversely affected by high discharges, a conclusion based on their inferred decrease in mortality rates during high-discharge years. This result also is consistent with the observation that mussels are spatially concentrated in areas of the channel protected from high flows (Howard and Cuffey 2003). One explanation for lower mortality in high-discharge years is related to scour of fine sediments. High flows may be necessary to remove silt and biological deposits that accumulate in mussel aggregations. These accumulations are particularly problematic in low-discharge refuges because silt may clog gills, reduce feeding efficiency, and reduce survival (Kat 1982, Brim Box and Mossa 1999). Accumulated silts also may reduce individual development and growth. Hruska (1992) found that individuals reared on clean gravels exhibited more consistent growth than individuals held in silty substrates. Thus, scouring floods may be necessary to maintain suitable mussel habitat and growth.

Between-river comparisons of mussel abundances and age structures

The striking difference in *M. falcata* abundance and age structure between the South Fork Eel and Navarro populations may be a consequence of: 1) the interplay of 2 interrelated factors, landuse history and fish populations, 2) the severe declines in the Navarro population after 1970 with little or no recruitment over the subsequent 30-y period, and 3) the important role that Q plays in shaping the age structure of the South Fork Eel population but not of the Navarro population.

Unlike the South Fork Eel, the Navarro has been impaired by a history of land uses in the watershed that has compromised its ecological integrity. Sediment loads and stream temperatures in much of the Navarro have been above Clean Water Act standards since the mid 1990s (USEPA 2000). Moreover, surveys by the California Department of Fish and Game conducted since the early 1960s have shown that salmonid spawning habitat in the North Fork Navarro has been significantly degraded, primarily from logging. Most of the North Fork Navarro was logged before 1945 and again after 1974 (USEPA 2000). Quantitative data are not available for host fish populations, but anecdotal evidence between 1920 and 1970 suggests that the Navarro was a popular fishing river with restaurants and hotels catering to anglers (Adams 2001). By 1980, these facilities were closed, and the Navarro fishery had collapsed. In contrast, the South Fork Eel mussel populations were in a relatively pristine reach entirely within protected lands where fish populations do not appear to be in decline (M. E. Power, University of California, unpublished data).

In summary, our study provides a powerful method to analyze factors influencing the population age structure of freshwater mussels. Similar models and techniques can be applied to mussel populations in other watersheds to provide a basic understanding of factors controlling demographics and to assist in conservation of this and other endangered mussels.

Acknowledgements

We thank the University of California Natural Reserve for protecting the Angelo Coast Range Reserve for research and teaching. We are indebted to Mary Power for allowing us use of her laboratory for processing, for guidance and wisdom, and for providing a stimulating research environment. We thank Mary Power, Jayne Brim Box and 2 anonymous referees for helpful comments on the manuscript and Peter Steel for logistical support. This research was supported by a grant from the California Center for Water Resources (#24924).

Literature Cited

Aberg, G., T. Wickman, and H. Mutvei. 1995. Strontium isotope ratios in mussel shells as indicators of acidification. Ambio 24:265–268.

Adams, H. 2001. What is the fate of the Navarro? The Eel River Reporter 4:3–6.

Bauer, G. 1983. Age structure, age specific mortality rates and population trend of the freshwater pearl mussel (*Margaritifera margaritifera*) in North Bavaria. Archiv für Hydrobiologie 98:523–532.

Bauer, G. 1992. Variation in the life span and size of the freshwater pearl mussel. Journal of Animal Ecology 61: 425–436.

BAUER, G., AND C. VOGEL. 1987. The parasitic stage of the freshwater pearl mussel (*Margaritifera margaritifera* L.) I. Host response to glochidiosis. Archiv für Hydrobiologie 4:393–402.

BEASLEY, C. R., AND D. ROBERTS. 1999. Assessing the conservation status of the freshwater pearl mussel in the north of Ireland—relevance of growth and age characteristics. Journal of Conchology 36:53–61.

BRIM BOX, J. 1999. Community structure of freshwater mussels (Bivalvia: Unionidae) in Coastal Plain streams of the Southeastern United States. PhD Dissertation, University of Florida, Gainesville, Florida.

BRIM BOX, J., AND J. MOSSA. 1999. Sediment, land use, and freshwater mussels: prospects and problems. Journal of the North American Benthological Society 18:99–117.

BRIM BOX, J., AND J. D. WILLIAMS. 1999. Unionid mollusks of the Apalachicola Basin in Alabama, Florida and Georgia. Bulletin of the Alabama Museum of Natural History 21: 1–156.

BUTLER, R. S. 1989. Distributional records of freshwater mussels (Bivalvia: Unionidae) in Florida and south Alabama with zoogeographic and taxonomic notes. Walkerana 3:239–261.

CAPPUCCINO, N., AND P. W. PRICE. 1995. Population dynamics: new approaches and synthesis. Academic Press, San Diego, California.

CARELL, B., S. FORBERG, E. GRUNDELIUS, L. HENRIKSON, A. JOHNELS, U. LINDH, H. MUTVEI, M. OLSSON, K. SVARDSTROM, AND T. WESTERMARK. 1987. Can mussel shells reveal environmental history? Ambio 16:2–10.

CASWELL, H. 2001. Matrix population models: construction, analysis, and interpretation. Sinauer Associates, Sunderland, Massachusetts.

COKER, R. E., A. F. SHIRA, H. W. CLARK, AND A. D. HOWARD. 1921. Natural history and propagation of freshwater mussels. Bulletin of the United States Bureau of Fisheries 37:75–181.

DAY, M. E. 1984. The shell as a recording device: growth record and shell ultrastructure of *Lampsilis radiata radiata* (Pelecypoda: Unionidae). Canadian Journal of Zoology 62:2495–2504.

DILLON, R. T. 2000. The ecology of freshwater molluscs. Cambridge University Press, Cambridge, UK.

ENTRIX, PACIFIC WATERSHED ASSOCIATES, CIRCUIT RIDER PRODUCTIONS, NAVARRO WATERSHED COMMUNITY ADVISORY GROUP, AND D. T. SICULAR. 1998. Navarro watershed restoration plan. Published jointly by Anderson Valley Land Trust, Coastal Conservancy, and Mendocino County Water Agency, Boonville, Oakland, and Ukiah, California, respectively. (Available from http://www.krisweb.com/biblio/navarro_mcwa_entrix_1998_restplan.pdf)

FULLER, S. 1974. Clams and mussels (Mollusca: Bivalvia). Pages 215–273 *in* C. W. Hart and S. L. H. Fuller (editors). Pollution ecology of freshwater invertebrates. Academic Press, New York.

GIANNICO, G. R., AND M. C. HEALEY. 1998. Effects of flow and food on winter movements of juvenile coho salmon. Transactions of the American Fisheries Society 127:645–651.

HASTIE, L. C., P. J. BOON, M. R. YOUNG, AND S. WAY. 2001. The effects of a major flood on an endangered freshwater mussel population. Biological Conservation 98:107–115.

HASTIE, L. C., M. R. YOUNG, AND P. J. BOON. 2000a. Growth characteristics of freshwater pearl mussels, *Margaritifera margaritifera*. Freshwater Biology 43:243–256.

HASTIE, L. C., M. R. YOUNG, P. J. BOON, P. J. COSGROVE, AND B. HENNINGER. 2000b. Sizes, densities, and age structures of Scottish *Margaritifera margaritifera* (L.) populations. Aquatic Conservation: Marine and Freshwater Ecosystems 10:229–247.

HENDELBERG, J. 1961. The freshwater pearl mussel, *Margaritifera margaritifera*. Journal of Conchology 29:207–218.

HOWARD, J. K. 2004. Freshwater mussels in California Coast Range rivers: abiotic controls and functional role. PhD Dissertation, Department of Geography, University of California, Berkeley, California.

HOWARD, J. K., AND K. M. CUFFEY. 2003. Freshwater mussels in a California North Coast Range river: occurrence, distribution, and controls. Journal of the North American Benthological Society 22:63–77.

HOWARD, J. K., K. M. CUFFEY, AND M. SOLOMON. 2005. Toward using *Margaritifera falcata* as an indicator of base level nitrogen and carbon isotope ratios: insights from two California Coast Range rivers. Hydrobiologia 541:229–236.

HRUSKA, J. 1992. The freshwater pearl mussel in South Bohemia: evaluation of the effect of temperature on reproduction, growth and age structure of the population. Archiv für Hydrobiologie 126:181–191.

KARNAT, D. W., AND R. E. MILLEMANN. 1978. Glochidiosis of salmonid fishes. Comparative susceptibility to natural infection with *Margaritifera margaritifera* and associated histopathology. Journal of Parasitology 64:528–537.

KAT, P. W. 1982. Effects of population density and substratum type on growth and migration of *Elliptio complanata* (Bivalvia: Unionidae). Malacological Review 15:119–127.

KINGSLAND, S. E. 1995. Modeling nature: episodes in the history of population ecology. University of Chicago Press, Chicago, Illinois.

KUPFERBERG, S. J. 1996. Hydrologic and geomorphic factors affecting conservation of a river-breeding frog (*Rana boylii*). Ecological Applications 6:1332–1344.

MCMAHON, T. E., AND G. F. HARTMAN. 1989. Influence of cover complexity and current velocity on winter habitat use by juvenile Coho salmon (*Oncorhynchus kisutch*). Canadian Journal of Fisheries and Aquatic Sciences 46:1551–1557.

MENKE, W. 1989. Geophysical data analysis: discrete inverse theory. Academic Press, San Diego, California.

NEVES, R. J., A. E. BOGAN, J. D. WILLIAMS, S. A. AHLSTEDT, AND P. W. HARTFIELD. 1997. Status of aquatic mollusks in the southeastern United States: a downward spiral of diversity. Pages 44–86 *in* G. W. Benz and D. E. Collins (editors). Aquatic fauna in peril: the southeastern perspective. Special Publication 1, Southeast Aquatic Research Institute. Lenz Design and Communications, Decatur, Georgia.

NEVES, R. J., AND S. N. MOYER. 1988. Evaluation of techniques for age determination of freshwater mussels (Unionidae). American Malacological Bulletin 6:179–188.

NOTT, M. P., E. ROGERS, AND S. PIMM. 1995. Modern extinctions in the kilo-death range. Current Biology 5:14–17.

NYSTROM, J., E. DUNCA, H. MUTVEI, AND U. LINDH. 1996. Environmental history as reflected by freshwater pearl mussels in the River Vramsan, Southern Sweden. Ambio 25:350–355.

OLI, M. K. 2003. Partial life-cycle models: how good are they? Ecological Modelling 169:313–325.

PRESS, W. H., S. A. TEUKOLSKY, W. T. VETTERLING, AND B. P. FLANNERY. 1992. Numerical recipes in FORTRAN: the art of scientific computing. Cambridge University Press, New York.

RENSHAW, E. 1991. Modelling biological populations in space and time. Cambridge University Press, Cambridge, UK.

STOBER, Q. J. 1972. Distribution and age of *Margaritifera margaritifera* (L.) in a Madison River (Montana, U.S.A.) mussel bed. Malacologia 11:343–350.

TAYLOR, D. W. 1981. Freshwater mollusks of California: a distributional checklist. California Fish and Game 67: 140–163.

TOY, K. A. 1998. Growth, reproduction and habitat preference of the freshwater mussel *Margaritifera falcata* in western Washington. MSc Thesis, University of Washington, Seattle, Washington.

USEPA (US ENVIRONMENTAL PROTECTION AGENCY). 2000. Navarro River total maximum daily loads for temperature and sediment. Report No. 10069. Region 9, US Environmental Protection Agency, San Francisco, California. (Available from: http://www.epa.gov/region09/water/tmdl/final.html)

WESTERN REGIONAL CLIMATE CENTER. 2002. Classification of El Niño and La Niña winters. Desert Research Institute, Reno, Nevada. (Available from: http://www.wrcc.dri.edu/enso/ensodef.html)

WILLIAMS, J. D., M. L. WARREN, K. S. CUMMINGS, J. L. HARRIS, AND R. J. NEVES. 1992. Conservation status of freshwater mussels of the United States and Canada. Fisheries 18(9):6–22.

YEAGER, M. M., D. S. CHERRY, AND R. J. NEVES. 1994. Feeding and burrowing behaviors of juvenile rainbow mussels, *Villosa iris* (Bivalvia:Unionidae). Journal of the North American Benthological Society 13:217–222.

YOUNUS, M., M. HONDZO, AND B. A. ENGEL. 2000. Stream temperature dynamics in upland agricultural watersheds. Journal of Environmental Engineering 126:518–526.

Received: 21 July 2004
Accepted: 8 May 2006

APPENDIX 1. Singular Value Decomposition.

The coefficient vector a_k from Nj^{modeled} (eq. 5) was perturbed by an initial arbitrary amount, da_k (in this case 0.1), and the result was used to calculate a gradient matrix (**G**), defined as:

$$\mathbf{G}_{jk} = \left[Nj^{\text{modeled}}(a_{k0} + da_k) - Nj^{\text{modeled}}(a_{k0} - da_k)\right]/(2da_k)$$

where j is the row corresponding to the specific data point, k is the column corresponding to the model parameter, and N_j is the number of individuals in the j^{th} row. In Analysis 1, the $j \times k$ matrix **G** was a 40×3 matrix, whereas in Analysis 2, it was a 40×4 matrix. Our goal was to find the vector of perturbation sizes da_k that minimized (by least squares) the mismatch between N^{modeled} and N^{measured}. This step was done iteratively using:

$$(Nj^{\text{modeled}} - Nj^{\text{measured}}) = (\mathbf{G}_{jk})(da_k)$$

and inverting $\mathbf{G}_{jk}$ using Singular Value Decomposition. This step provided the perturbation vector (da_k) that minimized J. We recalculated N_j^{modeled} using $ak = a_{k0} + da_k$.

APPENDIX 2. Calculation of discharge (Q).

We used discharge data from the US Geological Survey (USGS) records of daily stage measurements at the study site from 1946–1970 (Branscomb station). Recording of river stage was resumed in 1990 by M. E. Power, University of California, Berkeley, at the same staff gauge. We estimated Q from stage height using a rating curve provided by USGS (Kupferberg 1996). We estimated gaps in the record between 1970 and 1990 using data collected from a USGS gauging station (Leggett) ~35 km downstream of the Branscomb gauge. We correlated stage-height data at the Branscomb site with data at the Leggett site. We fitted a linear model to predict missing stage-height data at the Branscomb gage from the Leggett data (y = 0.19x – 10.67, $r^2 = 0.97$).